

# Influence of solid phase conductivity on spatial localization of electrochemical processes in flow-through porous electrodes

## Part I: Electrodes with uniform conducting matrix

A. I. MASLIY, N. P. PODDUBNY

*Institute of Solid State Chemistry, Siberian Branch of Russian Academy of Sciences, Novosibirsk, Russia*

Received 27 March 1996; revised 10 December 1996

Mathematical simulation of the flow-through porous electrode (PE) operation on the basis of a one-dimensional model with a uniform conducting matrix and a cathodic process involving the main and side reactions (i.e., hydrogen evolution) has been made. The influence of current density and rate and direction of the solution flow on the depth of the main process penetration into the PE has been analysed for different relationships between phase conductivities. It has been shown that when the polarization curve of the side reaction is Tafelian, and the rate of solution circulation is high, there is a limit for the main process penetration into the PE. This limiting value is close to the thickness of the layer,  $L_d$ , capable of working at the limiting diffusion current obtained by Sioda's method. The dependence of the  $L_d$  layer thickness on phase conductivity has been analysed. In the limiting cases (low fractional conversion, high or identical phase conductivities) analytical expressions for  $L_d$  have been obtained. At low flow rates, the depth of the main process penetration increases up to the value of the entire thickness of the PE. It can be concluded that the possibility of increasing the PE efficiency for the uniform matrix by changing phase conductivities is limited.

Keywords: *Solid phase conductivity, Flow-through porous electrodes, Electrode modelling*

### Nomenclature

$P(x), \varphi(x)$	local potentials in the solid and liquid phases (V)	$z$	number of electrons transferred per ion discharged in the main reaction
$\eta(x)$	polarization (V)	$F$	Faraday constant ( $96487 \text{ C mol}^{-1}$ )
$i, i_\ell$	local and limiting current densities ( $\text{A cm}^{-2}$ )	$L$	thickness of PE (cm)
$i_1, i_2$	current densities of the main and side reactions ( $\text{A cm}^{-2}$ )	$L_d$	thickness of PE layer operating at the limiting diffusion current (cm)
$i_a, i_g$	modulus of average and total (geometric) current densities ( $\text{A cm}^{-2}$ )	$L_{\text{eff}}$	effective value of $L_d$ involving the zones of current density lower than limiting (cm)
$i_{a\ell}, i_{g\ell}$	limiting values of modulus of the average and geometric current densities, when the entire PE surface is working at the limiting diffusion current ( $\text{A cm}^{-2}$ )	$X_{\text{min}}, X_{\text{max}}$	coordinates of points with the minimum and maximum polarization inside PE (cm)
$\phi_{r1}, \phi_{r2}$	equilibrium potentials of the main and side reactions (V)	$\Delta\eta_1, \Delta\eta_2$	polarization differences between the least loaded point inside PE and the back or frontal ends of the electrode (V)
$i_{01}, i_{02}$	exchange current densities ( $\text{A cm}^{-2}$ )	$\Delta\eta$	maximum value of polarization differences
$\alpha_1$	transfer coefficient of the main reaction	$\Delta E_1, \Delta E_2$	width of the limiting current plateau obtained by different ways of geometrical transformation of the total polarization curve
$k_m$	mass transfer coefficient ( $\text{cm s}^{-1}$ )	$R$	fractional conversion of the electroactive component
$\kappa_s, \kappa_L$	solid and liquid phase conductivities ( $\Omega^{-1} \text{ cm}^{-1}$ )	$R_1 = 1/\kappa_s + 1/\kappa_L$	
$S_v$	specific surface of the PE ( $\text{cm}^{-1}$ )	$R_2 = \kappa_L/(\kappa_s + \kappa_L)$	
$C, C_s$	local concentrations of the electroactive component inside a pore and at the surface of the PE ( $\text{mol cm}^{-3}$ )	$A_1 = C_0 z F u$	
$u$	linear rate of the solution flow ( $\text{cm s}^{-1}$ )	$A = S_v k_m L/u$	
		$B = A/L$	

## 1. Introduction

The application of porous electrodes (PE) of high specific surface area and mass transfer coefficient is a promising approach to electrochemical process intensification. At present, PE are commonly used in chemical power supplies, fuel cells and metal extraction from industrial solutions and waste waters [1–3]. The main problem in PE theory is the search for conditions providing the most efficient utilization of their extended surface for the performance of the specified main process. These conditions commonly involve attainment of the most uniform potential distribution over the PE depth and depend on several factors. The influence of electrochemical factors associated with the electrode–solution interface have received most attention [4–7]. The parameters that determine the passage of the current over the solid and liquid phases have been considered as passive factors (i.e., as constants) and have not yet been used for active control of the spatial localization of electrochemical processes.

In most work on PE theory, the solid phase conductivity is assumed to be constant (more often  $\kappa_s(x) = \infty$ ). Nevertheless, the necessity of considering the  $\kappa_s(x)$  profile to interpret the observed current distribution over a PE may be illustrated by the following examples. First, solid-phase conductivity changing with electrode thickness has been observed experimentally; for example, in metal electrodeposition on high-resistance porous matrices. Solid-phase conductivity determines, to a great extent, practically important parameters for filling the matrices with metal [8]. Second, it is difficult to explain anomalous phenomena such as the appearance of anodic zones inside cathodic polarized PEs without considering solid and liquid phase conductivity profiles occurring inside the PE [9]. Third, approximate theoretical estimates show that the varying profile of solid-phase conductivity holds much promise for smoothing current distribution to the point of it being ideally uniform [10].

Taking into account the above considerations, an attempt is made to follow the main tendencies and quantitative scales of the influence of solid-phase resistance on the spatial localization of the main electrochemical process and, eventually, on the efficiency of PE internal surface utilization. Since the action of factors determining the electric field in a PE is often interconnected, the influence of one factor depends on the changes of the others. Therefore, in discussing the influence of the solid phase we shall partly consider the influence of other parameters such as liquid-phase resistance, solution flow rate, electrode thickness and current density.

## 2. Physical and mathematical formulation of the problem

The main method of analysis used in the present paper is numerical simulation of PE performance

based on the computation of electric and concentration fields inside the PE with the adoption of a definite physical model and kinetic equations for the total polarization curve. By analysing the current and potential distribution across the PE, it is possible to determine the quantitative characteristics of the performance efficiency (i.e., layer thickness working at the limiting diffusion current) and observe their dependence on different parameters.

To avoid unnecessary mathematical difficulties, we use the simplest unidimensional mathematical model of a PE (Fig. 1) and the simplest electrode process involving the main and side (hydrogen evolution) electrochemical reactions. For definition, it should be also mentioned that the PE under consideration has a back current feeder to which the origin of coordinates is fixed. The X-axis is directed inside the PE to a counter electrode.

The mathematical model [4, 7, 9] is based on the simultaneous solution of a differential equation for the potential and current distribution and a transfer equation for the discharging ion of the main reaction. For constant  $\kappa_s$  and  $\kappa_L$ ,

$$d^2\eta/dx^2 = S_v R_1 i(\eta) \quad (1)$$

$$dc/dx = S_v i_1(\eta - \phi_{r1}) / (u z F) \quad (2)$$

where

$$\eta(x) = P(x) - \phi(x) \quad (3)$$

$$i(\eta) = i_1(\eta - \phi_{r1}) + i_2(\eta - \phi_{r2}) \quad (4)$$

Since we consider the case of large differences of concentration gradients, it is reasonable to account for the concentration dependence of  $\phi_{r1}$  using the Nernst equation.

$$\phi_{r1} = \phi_{r0} + \frac{RT}{zF} \ln c(x) \quad (5)$$

where  $\phi_{r0}$  is the standard value of  $\phi_{r1}$ .

To solve this set of simultaneous equations, the following boundary conditions are used:

at  $x = 0$ ,  $c = c_0$

$$d\eta/dx = i_g/\kappa_s \quad (6)$$

at  $x = L$

$$d\eta/dx = -i_g/\kappa_L \quad (7)$$

where

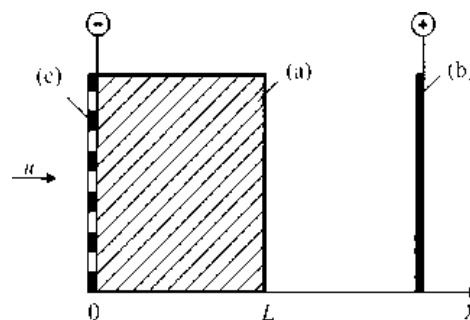


Fig. 1. Relative positions of working (a) and counter (b) electrodes, current-feeder (c) and the direction of current flow.

$$i_g = L i_a S_v \quad (8)$$

We consider a cathodic process, so that at  $L > x > 0, \eta < 0$  and  $i(\eta) < 0$ . The absolute values of the geometric current density in Equations 1, 6, 7 and of the average current density in Equation 8 are taken; thus they are positive. A partial polarization curve of the main process takes into account the discharge transfer stage and concentration changes in the surface layer of solution:

$$i_1 = i_{01} \left( \exp\left(\frac{\alpha z F}{RT}(\eta - \phi_{r1})\right) - \frac{c_s(x)}{c(x)} \exp\left(-\frac{(1-\alpha)zF}{RT}(\eta - \phi_{r1})\right) \right) \quad (9)$$

In the steady state:

$$c_s(x)/c(x) = 1 - i_1/i_{1\ell} \quad (10)$$

where

$$i_{1\ell} = z F c(x) k_m \quad (11)$$

and  $k_m$  is the mass-transfer coefficient which depends on the flow rate [11]:

$$k_m = 0.02 u^{0.35} \quad (12)$$

Equation 10 allows  $i_1$  to be expressed as a function of  $i_{1\ell}$  and  $\eta$ .

$$i_1 = \frac{i_{01} \left( \exp\left(\frac{\alpha z F}{RT}(\eta - \phi_{r1})\right) - \exp\left(-\frac{(1-\alpha)zF}{RT}(\eta - \phi_{r1})\right) \right)}{\left( 1 + \frac{i_{01}}{i_{1\ell}} \exp\left(-\frac{(1-\alpha)zF}{RT}(\eta - \phi_{r1})\right) \right)} \quad (13)$$

Only the discharge stage is considered in the partial cathodic polarization curve of hydrogen evolution:

$$i_2 = i_{02} \left( \exp\left(\frac{F}{2RT}(\eta - \phi_{r2})\right) - \exp\left(-\frac{F}{2RT}(\eta - \phi_{r2})\right) \right) \quad (14)$$

$\phi_{r2}$  is assumed to be constant, and the transfer coefficient is taken to be 0.5.

The method used in the calculations was similar to that described in [7], with the following additional criteria of solution stability [12]: (a) an integral of the current density along the thickness of the PE must be equal to the given total current to a sufficient accuracy (of 1%); and (b) a solution must be stable with doubling the number of grid points over the depth of the PE.

It should also be noted that for a uniform porous matrix, a simpler method of calculation suggested by Sioda [13] fits adequately. The principle of this method is based on the fact that the common problem of calculating the current and potential distribution over a PE is reduced to the search for a maximum polarization difference between points assuming that the entire PE surface is working at the limiting current. This allows consideration of the diffusion component of the equation describing current transfer, which simplifies further analysis significantly and, in some cases, helps to obtain

analytical solutions. We shall also use this approach, extending it to include arbitrary relations between phase conductivities.

### 3. Results and discussion

#### 3.1. Symmetry of electrical and concentration fields in a PE

The boundary problem described above has variations according to the relations between the solid and liquid phase conductivities, the location of the current-feeder and the direction of the solution flow (see, for example, [6]). A complete consideration of the variants involves a large body of numerical calculations. However, the latter may be significantly reduced without any significant loss of analysis completeness by taking into account the symmetry of the boundary problem.

The boundary problem (Equations 1–7) has been deduced for back solution supply. For the front supply, Equation 1 will be invariant to the change of the direction of the X-axis for the opposite. Equation 2 will be invariant to the reversal of both X-axis and flow direction. If the  $\kappa_s$  and  $\kappa_L$  values change places in the boundary conditions, the same boundary problem is obtained; that is, the system possesses symmetry about the supply direction and solid and liquid-phase conductivities. Evidence for this symmetry has been obtained earlier for the case of high solution flow rates [14].

Due to the symmetry, the electrical and concentration fields in the PE for back supply and definite  $\kappa_s$  and  $\kappa_L$  values are completely identical to the corresponding fields for front supply and opposite  $\kappa_s$  and  $\kappa_L$  values. Therefore, it is sufficient to study the behaviour of different parameters for only one of the two supply variants (for example, the back one) over a wide range of both phase conductivities.

#### 3.2. $L_d$ estimate for arbitrary relation between solid and liquid phase conductivities

Quantitative analysis of  $L_d$  has been carried out in [13] for back solution supply and infinite conductivity of the solid matrix. In this case, the polarization distribution over the depth of the PE is monotonic, and the required difference in the maximum and minimum values of polarization has been determined by integrating over the entire depth of the electrode,  $L$ . An attempt to extend the results of [13] to the case of an arbitrary relation of phase conductivities has been made [15]. However, nonmonotony of the current distribution over the depth of the electrode has not been accounted for, which has led to erroneous results.

To determine the maximum abrupt change of the diffusion polarization, it is necessary first to find the position of its minimum. The Equation 1 is to be integrated between 0 and  $x$ . In this case, it should be

considered that  $i(x) = i_{1\ell}(x)$ , that is, the local current density is equal to its diffusion component, and the geometric density of the limiting diffusion current  $i_{g\ell}$  is expressed as

$$i_{g\ell} = \int_0^L i_{1\ell} S_V dx = A_1(1 - \exp(-A)) \quad (15)$$

Taking into account that  $d\eta/dx = 0$  at the point of minimum, after substitution of Equation 15 and some transformations we obtain

$$\frac{x_{\min}}{L} = -\frac{1}{A} \ln[1 - R_2 + R_2 \exp(-A)] \quad (16)$$

It follows from Equation 16 that the relative position of the minimum concentration polarization is determined by two dimensionless complexes, namely, the relation between the solid and liquid-phase conductivities and a parameter,  $A$ , which evaluates the extent to which the electroactive component concentration is reduced as the solution passes through the PE. This dependence is shown in Fig. 2. It is clear that for small  $A$ , that is, for small fractional conversion, the position of  $x_{\min}$  depends only on the relation  $\kappa_s/\kappa_L$ : for  $\kappa_s = \kappa_L$ ,  $x_{\min} = 0.5L$ ; for  $\kappa_s \ll \kappa_L$ ,  $x_{\min} \rightarrow L$ ; for  $\kappa_s \gg \kappa_L$ ,  $x_{\min} \rightarrow 0$ . For high values of  $A$  (fractional conversion of electroactive component per a passage of the solution is about 1), the position of the minimum point is independent of the relation between the conductivities and coincides with the point where the most concentrated solution is introduced into the PE ( $x = 0$ ). For the intermediate range of  $A$ , the position of  $x_{\min}$  is determined by the complexes both simultaneously.

Thus, knowing the position of the polarization minimum and alternately integrating Equation 1 between 0 and  $x_{\min}$ , and between  $x_{\min}$  and  $L$ , we obtain expressions for potential differences between this point and the back and front ends of the PE, respectively:

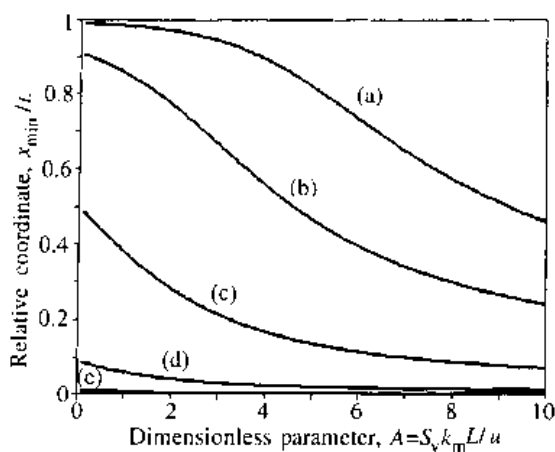


Fig. 2. Relative coordinate of the polarization minimum inside PE against the value of the dimensionless parameter  $A$  at the back solution supply and the following values of  $\kappa_s/\kappa_L$ : (a) 0.01; (b) 0.1; (c) 1; (d) 10; (e) 100.

$$\begin{aligned} \Delta\eta_1 &= \eta(x_{\min}) - \eta(0) \\ &= \frac{i_{g\ell} x_{\min}}{\kappa_s} - R_1 A_1 x_{\min} - \frac{R_1 A_1}{B} [\exp(B x_{\min}) - 1] \end{aligned} \quad (17)$$

$$\begin{aligned} \Delta\eta_2 &= \eta(L) - \eta(x_{\min}) \\ &= \frac{i_{g\ell}(L - x_{\min})}{\kappa_s} - R_1 A_1 (L - x_{\min}) \\ &\quad - \frac{R_1 A_1}{B} [\exp(-A) - \exp(-B x_{\min})] \end{aligned} \quad (18)$$

The largest of these differences  $\Delta\eta$  determines the maximum thickness  $L_d$  of a PE capable of working at the limiting diffusion current. Equating it to the width,  $\Delta E$ , of the limiting current plateau on the polarization curve, we obtain a transcendental equation with respect to  $L_d$ , which may be solved by an appropriate numerical method, for example, by dividing the length in two. From Equations 17 and 18 it follows that, as opposed to the position of the minimum polarization point, the value of  $L_d$  depends not only on the relationship between the solid and liquid-phase conductivities, but also on their absolute values. The three-dimensional surface  $L_d = f(\kappa_s, \kappa_L)$  would be a clear illustration of this dependence. The sections of this surface at  $\kappa_s = \text{const}$  and  $\kappa_L = \text{const}$  obtained at constant  $\Delta\eta$  and PE parameters for a range of linear solution rates, are shown in Figs 3 and 4, respectively. The values of solution rates are chosen so as to demonstrate the influence of different fractional conversion of the electroactive component. It is evident from Fig. 3 and 4 that in the general case  $L_d$  is a composite function of the solid and liquid-phase conductivities. The main features of this dependence are as follows:

- (i) At any solution flow rate a decrease in the phase conductivity of both solid (Fig. 3) and liquid (Fig. 4) phases leads to a decrease in  $L_d$  down to zero. Such a behaviour of  $L_d$  seems to be natural

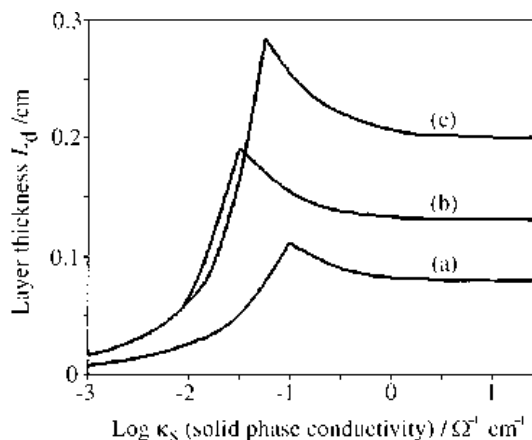


Fig. 3. The maximum PE depth working at the limiting diffusion current as a function of the solid phase conductivity at different solution flow rates ( $\text{cm s}^{-1}$ ): (a) 10; (b), (c) 0.2 and the definite values of  $\kappa_L$  ( $\Omega^{-1} \text{cm}^{-1}$ ): (a), (c) 0.1; (b) 0.05. The back solution flow; other parameters:  $c_{01} = 10^{-5} \text{M cm}^{-3}$ ,  $z = 1$ ,  $S_V = 150 \text{cm}^{-1}$ ,  $\Delta\eta = 0.3 \text{V}$ .

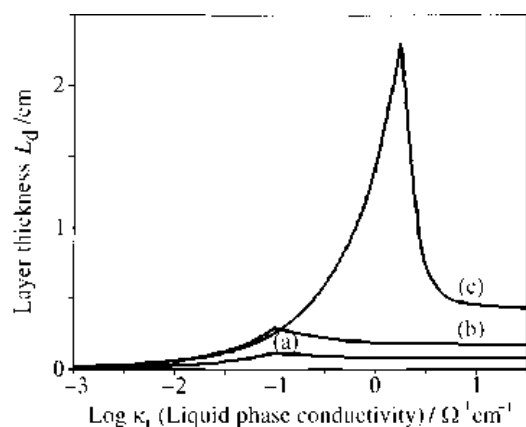


Fig. 4. Examples of sections of the surface  $L = f(\kappa_s, \kappa_L)$  by the planes  $\kappa_s = \text{const}$  ( $\Omega^{-1} \text{cm}^{-1}$ ): (a), (c) 0.1; (b) 0.05; at different solution flow rates ( $\text{cm s}^{-1}$ ): (a) 10; (b), (c) 0.2. Other parameters are the same as in Fig. 3.

because in both these boundary cases the electrode ceases to be permeable to the current.

- (ii) At high solid and liquid-phase conductivities,  $L_d$  tends to a limit essentially dependent on the solution rate.
- (iii) Between the above-mentioned boundary values, the dependence  $L_d = f(\kappa_s, \kappa_L)$  has a maximum which corresponds to the equality  $\kappa_s = \kappa_L$  at high solution rate. Under these conditions the influence of  $\kappa_s$  and  $\kappa_L$  is completely symmetrical (see curves (a) in Figs 3 and 4).

**3.2.1. Approximate analytical equations.** At low values of the dimensionless parameter  $A$  and given values of phase conductivities, approximate analytical expressions for  $L_d$  may be deduced. An approximate relation for the minimum polarization point may be initially derived. Replacing  $\exp(-A)$  in Equation 16 by  $(1 - A)$  and  $\ln(1 - R_2A)$  by  $-R_2A$ , We have

$$x_{\min}/L \cong R_2 = \kappa_L/(\kappa_s + \kappa_L) \quad (19)$$

With allowance for the known minimum position, we consider the approximate equality for  $L_d$  at specific relations between  $\kappa_s$  and  $\kappa_L$ .

- (a)  $\kappa_s \gg \kappa_L$  OR  $\kappa_s \ll \kappa_L$

At high conductivity of the electrode matrix, the minimum of polarization is near the back current-feeder. Therefore, the difference in potentials between the least and the most loaded points of PE is determined by Equation 18. Substituting  $\kappa_s = \infty$  and  $x_{\min} = 0$  in Equation 18 and changing  $\exp(-A)$  by expansion into a series to the third term  $(1 - A + A^2/2)$ , we obtain a relation for  $\Delta\eta$ , completely coinciding with that previously deduced for the same conditions [13, 16–19]:

$$\Delta\eta \cong \frac{A_1 AL}{2\kappa_L} \quad (20)$$

Thus, the thickness of PE capable of working at the limiting diffusion current can be estimated as follows:

$$L_{d, \kappa_s \rightarrow \infty} \cong \sqrt{\frac{2\kappa_L \Delta\eta}{A_1 B}} \quad (21a)$$

This relation gives a square root dependence of  $L_d$  on the electrode parameters and electrolysis conditions. At  $\kappa_L \rightarrow \infty$ , an analogous limit results:

$$L_{d, \kappa_L \rightarrow \infty} \cong \sqrt{\frac{2\kappa_s \Delta\eta}{A_1 B}} \quad (21b)$$

- (b)  $\kappa_s = \kappa_L$

In this case  $\Delta\eta_1 = \Delta\eta_2$ ,  $x_{\min} = L/2$ ,  $R_1 = 2/\kappa_L$ . Substituting these values into Equation 17 and replacing  $\exp(-Bx_{\min})$  by expansion into a series to the third term, gives the following equality for  $L_d$ :

$$L_{d, \kappa_s = \kappa_L} \cong \sqrt{\frac{4\kappa_L \Delta\eta}{A_1 B}} \quad (22)$$

It is evident that at equal phase conductivities, the square root dependence of  $L_d$  on PE parameters and electrolysis conditions remains valid. At equal values of the parameters, the PE thickness capable of working at the limiting diffusion current in this case should be  $\sqrt{2}$  times that for the infinite conductivity of, for example, the solid phase. Comparing the relationships between limiting values (Equations 21 and 22) with the data in Figs 3 and 4, they are in agreement with the results of numerical calculations.

### 3.3. Comparison of approximate $L_d$ estimates with the results of complete calculation of the current distribution over a PE: influence of average current density

Figure 5 shows an example of the cathodic polarization curve used in calculations and illustrates different graphic methods used in estimation of the

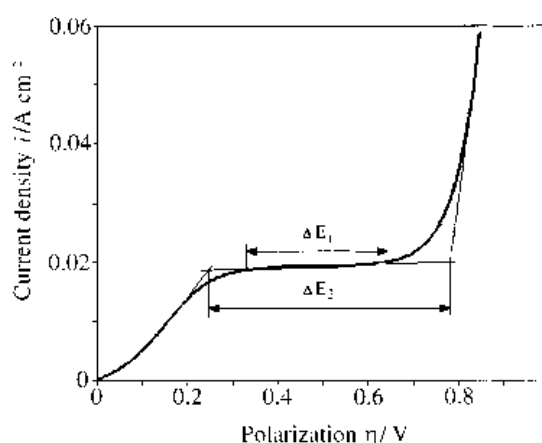


Fig. 5. An overall cathodic polarization curve of the main and side reactions and a scheme of two graphic methods providing the minimum ( $\Delta E_1 = 320 \text{ mV}$ ) and the maximum ( $\Delta E_2 = 530 \text{ mV}$ ) limiting current plateau width. The boundaries of the limiting current plateau are determined by the points where the current deviates from the limiting value by the given magnitude (1–2%) (1st method), and the points of crossing of the limiting current line with the tangents to partial polarization curves of the main and side reactions (2nd method). Parameters:  $c_{01} = 10^{-5} \text{ M cm}^{-3}$ ,  $i_{01} = 10^{-3} \text{ A cm}^{-2}$ ,  $\alpha_1 = 0.5$ ,  $z_1 = 1$ ,  $i_{02} = 10^{-6} \text{ A cm}^{-2}$ ,  $\phi_{12} - \phi_{11} = -0.3 \text{ V}$ ,  $u = 1 \text{ cm s}^{-1}$ .

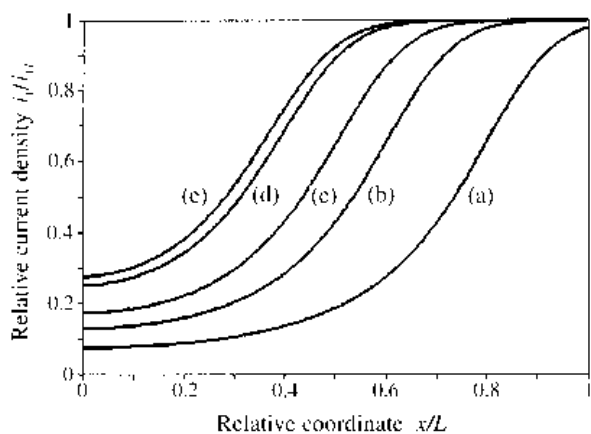


Fig. 6. Distribution of the relative current density of the main reaction over the depth of PE at different values of geometric current density ( $\text{A cm}^{-2}$ ): (a) 0.3; (b) 0.6; (c) 0.8; (d) 1; (e) 1.5. Parameters of PE:  $L = 0.5 \text{ cm}$ ;  $S_V = 150 \text{ cm}^{-1}$ ;  $\kappa_s = 100 \Omega^{-1} \text{ cm}^{-1}$ ;  $\kappa_L = 0.2 \Omega^{-1} \text{ cm}^{-1}$ . Other parameters are the same as in Fig. 5.

width of the limiting current plateau for the main reaction. It is clear that, depending on the methods, the plateau width ranges between 320 and 530 mV. In accordance with Equation 21(a), this corresponds to  $L_d$  values of 0.2 and 0.26 cm.

Figure 6 gives a typical variation pattern of the spatial localization of the main process over the depth of a sufficiently thick ( $L \approx 3L_d$ ) PE as the geometrical current density is changed. In order to clearly differentiate the parts of the electrode working at the limiting current, the relative current density  $i_1/i_{1l}$  is used. In this case, the parts of the PE where this ratio is equal to  $1 \pm 0.01$  correspond to the region of diffusion control. From the results shown in Fig. 6 it is evident that at low geometric current density, the limiting diffusion current is not attained even at the most loaded point of the electrode. Current distribution is very nonuniform and localized at the front end of PE. As the current density increases, the profile of current distribution for the main reaction moves deep into the electrode, but this is observed only until a certain limit is achieved. A further increase in the current load has essentially no effect on the profile of the  $i_1$  distribution.

As seen from Fig. 6, the working region of the electrode is not equivalent to the layer thickness  $L_d$  but is appreciably wider. Therefore, to characterize quantitatively the PE efficiency, it is appropriate to introduce, along with  $L_d$ , the effective thickness of the working region of the PE,  $L_{\text{eff}}$ , which accounts for the total current of the main reaction:

$$L_{\text{eff}} = \int_0^L \frac{i_1(x)}{i_{1l}(x)} dx \quad (23)$$

The changes of  $L_d$ ,  $L_{\text{eff}}$  and the current efficiency of the main reaction with the increase in the geometric current density are shown in Fig. 7. It is evident that both parameters of the spatial localization of the main process change analogously, which is a result of the approximate parallelism of the current profiles in Fig. 6. The deceleration of the movement of the working region deep into the electrode with increase

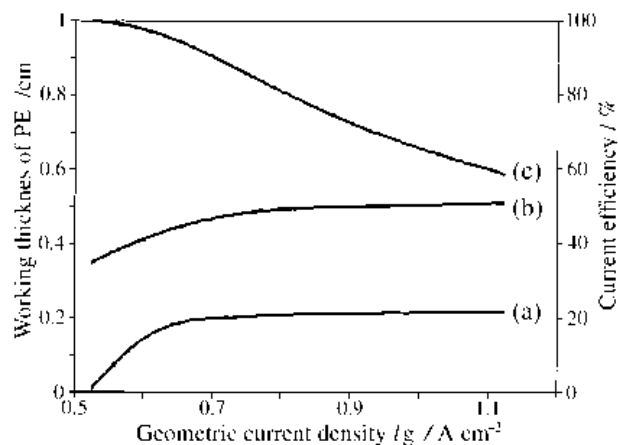


Fig. 7. The influence of geometric current density on the PE layer depth working at the limiting current  $L_d$  (a), the effective working layer depth  $L_{\text{eff}}$  (b) and the current efficiency of main reaction (c). The conditions are the same as in Fig. 6.

in geometric current density and the attainment of limiting values by both the parameters are apparently correlated with the marked decrease in the current efficiency. This means that the loaded region of the electrode is localized in the region of polarization corresponding to the hydrogen part of the polarization curve. As the current density increases further, essentially the whole additional current is spent on the useless (and taking into account possible side negative effects, rather harmful) hydrogen evolution in the PE and has no influence on the spatial localization of the main process.

Thus, the above results show that when the side cathodic process of hydrogen evaluation takes place, it is impossible to cause the main process to penetrate into the porous electrode deeper than to a certain limit by increasing the geometric current density. For example, under the conditions given in Fig. 6 at a total electrode thickness of 0.5 cm, the thickness of the limiting layer working at the limiting diffusion current, is 0.2 cm. Comparison of this value with  $L_d$  estimates by the Sioda method shows that it coincides with the value calculated from the minimum width of the limiting current plateau (0.2 cm). The employment of the maximum width of the limiting current plateau gives  $L = 0.26 \text{ cm}$  which is 30% above the true value.

In conclusion, in the above case the working surface of a PE available for the main reaction is independent of the geometric current density under conditions where the whole surface is not working at the limiting current. This means that such independence is a necessary, but not sufficient, condition for working of the entire PE thickness at the limiting diffusion current.

### 3.4. Influence of the rate and direction of solution flow on the efficiency of the PE

The direction and rate of solution flow through a PE is a significant electrolysis parameter controlling the electroactive component mass transfer [2], and also

the uniformity of the main reaction distribution over the depth of the PE [6, 14]. The simplest current distribution pattern is observed at high solution rates. Under these conditions, the electroactive component concentration changes insignificantly during its passage through the PE. Correspondingly, the polarization curve is one and the same at every point in the PE. Hence, the direction of solution flow turns out to be nonessential and the efficiency of the PE internal surface operation depends only on the potential distribution. A decrease in the solution flow rate may lead, as well as the qualitative changes in some parameters (for example, mass transfer coefficient), to the appearance of a new factor, that is, a profile of the electroactive component concentration over the depth of the PE. The interplay of the latter with the potential profile gives a more complicated current distribution pattern. Actually, at every point of the PE there is a distinct polarization curve which may differ from others not only by the height of the limiting current plateau but also by its width (due to the shift in the equilibrium potential). As a result, a choice of the plateau width and corresponding application of an approximate estimate of  $L_d$  in this case is more difficult. Therefore, to analyse the influence of the solution rate and direction, a set of complete calculations of the electric and concentration fields in a PE of fixed thickness ( $L = 1$  cm) was carried out for the polarization curve (Fig. 5) and a wide region of solution flow rates ( $u = 0.03 \div 30 \text{ cm s}^{-1}$ ) for three characteristic relationships between phase conductivities:  $\kappa_s \gg \kappa_L$ ,  $\kappa_s = \kappa_L$  and  $\kappa_s \ll \kappa_L$ . In view of the results of the previous Section concerning the dependence of the depth of the main process penetration on the average current density, all the calculations were conducted at the constant current overload  $i_a/i_{at} = 1.1$ . The layer thickness  $L_d$  working at the limiting diffusion current served as a quantitative measure of the PE efficiency.

Figure 8 presents the characteristic relations of  $L_d$  dependences on the solution flow rate. It can be seen that over a wide range of  $u$ , two parts of the plot differing by the steepness of the slope and the influence of the relationship between  $\kappa_s$  and  $\kappa_L$  are observed. At high solution flow rates,  $L_d$  depends on  $u$  only weakly and the boundary cases ( $\kappa_s \gg \kappa_L$  and  $\kappa_s \ll \kappa_L$ ) coincide completely. Moreover, at equal  $\kappa_s$  and  $\kappa_L$ , the thickness of the effective operating layer is about one and a half times larger, that is, the previously established regularities of the  $\kappa_s$  and  $\kappa_L$  influence are valid (see Section 3.2.1). A physical cause of  $L_d$  reducing with  $u$  rise (in this range of solution flow rates) is associated with the increasing height of the limiting current plateau due to the dependence of  $k_m$  on the flow rate.

For low solution flow rates ( $u < 0.5 \text{ cm s}^{-1}$ ), another picture is evident, that is,  $L_d$  increases abruptly with decreasing  $u$  and a considerable difference between the boundary cases ( $\kappa_s \gg \kappa_L$  and  $\kappa_s \ll \kappa_L$ ) is observed. Moreover, the advantages related to the equality of conductivities disappear and the curve for

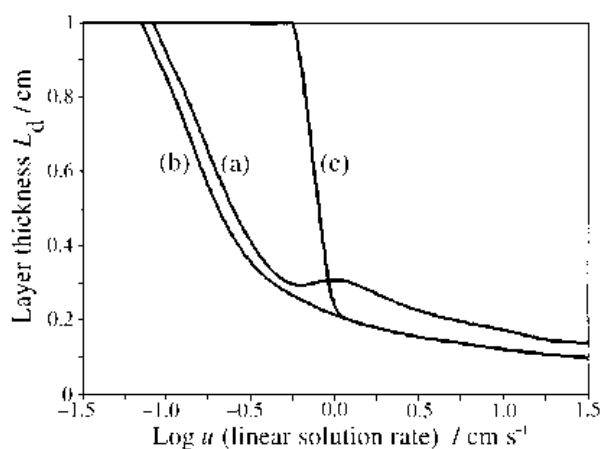


Fig. 8. The influence of the solution flow rate on the depth of PE layer working at the limiting diffusion current at different values of phase conductivities ( $\Omega^{-1} \text{ cm}^{-1}$ ): (a)  $\kappa_s = \kappa_L = 0.2$ ; (b)  $\kappa_s = 200$ ,  $\kappa_L = 0.2$ ; (c)  $\kappa_s = 0.2$ ,  $\kappa_L = 200$ . Characteristics of PE: the back current feeder, the back solution supply  $S_v = 150 \text{ cm}^{-1}$ ,  $L = 1$  cm. The parameters of the polarization curve are the same as in Fig. 5.

$\kappa_s = \kappa_L$  practically coincides with that for  $\kappa_s \gg \kappa_L$ . The curves reach a limit at even lower values of flow rate. This means that the PE width capable of working at the limiting current exceeds the value of  $L$ .

Obviously, the above-mentioned peculiarities of low solution rates in this range of  $u$  indicate the emergence of a new controlling factor which facilitates the penetration of the process into the PE. This factor is most likely to be the abrupt decrease in the electroactive component concentration over the depth of the electrode and the corresponding increase in the polarizability of the electrode. This conclusion is clearly confirmed by Fig. 9, where the same data for  $L_d$  as those given in Fig. 8 are shown as functions of fractional conversion  $R = 1 - c(L)/c(0)$ . It is evident that when the concentration change for a passage is small (about one order of magnitude), the width of the working layer is also small and depends on  $R$  only weakly. However, when  $R \rightarrow 1$ , the function  $L_d = f(R)$  becomes an essentially vertical line

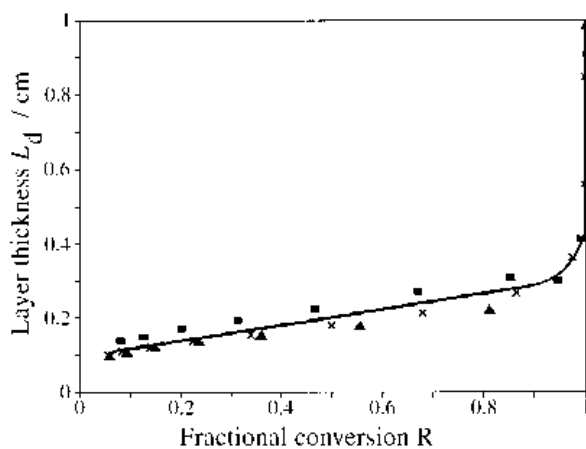


Fig. 9. The PE layer depth working at the limiting diffusion current against the fractional conversion of the electroactive component  $R$  (with data in Fig. 8). (■) variant (a); (▲) (b); (×) (c). The lines are simply fitted curves passing through the points.

and such a character of the dependence is observed for any relations between  $\kappa_s$  and  $\kappa_L$ .

The latter result is somewhat different from the conclusions of [6], where a principle difference in PE behaviour with  $\kappa_s \gg \kappa_L$  for back and front solution supply has been emphasized: for front supply, even a very thick PE ( $L_d > 15$  cm) is operating at the limiting diffusion current, but for back supply it is not ( $L_d < 2.5$  cm). Taking into account the previously established symmetry of the electrical field in a PE, a change in the direction of solution supply is equivalent to replacement of the relation between phase conductivities by the opposite one at the same solution supply. A noticeable difference between these variants is apparent from Fig. 8; however, it is quantitative rather than qualitative. At sufficiently low flow rate, the limiting current may be attained over the entire surface of the PE both at the front and at back supply, but in the latter case, lower values of  $u$  are needed.

A physical reason for the essential difference in PE efficiency for the reverse direction of solution supply at low flow rates seems to be the different interaction of polarization and electroactive component concentration profiles over the PE depth. When the mentioned profiles coincide in the character of behaviour ( $\kappa_s \ll \kappa_L$  with back supply) the most favourable conditions occur for the working of the entire surface at the limiting diffusion current. Actually, in this case the most loaded point (near the back current-feeder) and the point where the most concentrated solution enters the electrode coincide. When moving away from this point, an exponential drop in the main reaction current and approximately the same decrease in concentration are observed. Thus, the state of the limiting current is maintained as if automatically.

The most unfavourable situation occurs for the profiles  $\eta(x)$  and  $c(x)$  with the opposite character of behaviour, that is, the minimum solution concentration corresponds to the most loaded point of the PE, and vice versa. This makes the attainment of the limiting diffusion current over the entire PE surface difficult, but in this case, the depletion of the solution in the depth of PE also causes an increase in the polarization resistance at these points and current redistribution towards the less loaded layers. Eventually, this leads to the efficient working of the entire PE surface, but it is more costly (because of the lower solution flow rate, higher current overload and decrease in the current efficiency).

Relationships between the difference in the maximum and minimum values of polarization and the solution flow rate are shown in Fig. 10. These were calculated for the same variants as in Fig. 8. It is evident from the comparison of the figures that both the behaviour of  $L_d$  and polarization difference are closely interrelated. At high  $u$ , the potential differences at the most and the least loaded points are large, depend on  $u$  only weakly, and are equal for the boundary cases  $\kappa_s \gg \kappa_L$  and  $\kappa_s \ll \kappa_L$ . At low rates,

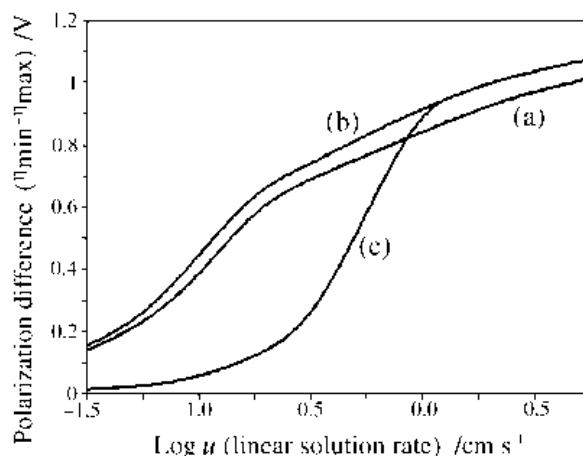


Fig. 10. The influence of the solution flow rate on the difference between the maximum and minimum polarization inside PE at the same parameters and notations as in Fig. 8.

the polarization difference tends to zero in all cases, and the most abrupt drop is observed for the similar profiles  $c(x)$  and  $\eta(x)$  which appears to provide a more efficient operation of the PE in this case.

### 3.5. Consideration of $\varphi_{r1}$ variability

The above results have been obtained with the proviso that the equilibrium potential of the main reaction is kept constant throughout the PE. It would be expected that at low  $u$  and the abrupt depletion of the solution, a shift of  $\varphi_{r1}$  of the local polarization curves in the negative region and the resulting reduction in the limiting current plateau may be essential factors. Just the same calculations, conducted with allowance for possible variability of  $\varphi_{r1}$ , have shown that as  $c(x)$  changes by even three to four orders per pass, the influence of this factor is practically absent. This is probably due to a decrease in the polarization difference with decreasing solution flow rate (Fig. 10). Only at a rather larger depletion extent (about 7–10 orders), significantly exceeding really available control limits, does the effect of  $\varphi_{r1}$  variability manifest itself and leads to the reduction in the PE layer width working at the limiting diffusion current.

## 4. Conclusion

The potential possibilities of the uniform porous matrix conductivity as a factor influencing the depth of the main process penetration into a PE have been estimated. The results suggest that these possibilities depend on the electrolysis conditions.

Thus, the most favourable conditions (a porous electrode similar to one with equal polarization, the highest values of  $L_d$ ) are observed only at very low solution flow rates and large difference in the electroactive component concentration along the depth of the PE. In this case, the optimum phase conductivity relation is that allowing achievement of a monotonic polarization profile similar to the main component concentration profile. It is apparent, however, that an



advantage in the working layer depth is obtained in this case due to the decrease in the solution flow rates and the productive capacity of the apparatus. Moreover, a sufficiently uniform potential distribution is accompanied, in this case, by the nonuniform current density distribution along the depth of the PE, which is extremely undesirable, for example, in the use of a PE for metal extraction from solutions. The nonuniform metal distribution along the depth of a layer leads to rapid filling of pores at the most loaded end of the electrode and to termination of its effective operation.

As the solution flow rate increases, the concentration difference decreases and an abrupt decrease in  $L_d$  and the working layer width is observed simultaneously. The value of the latter increases with decreasing concentration ( $\cong 1/\sqrt{c_0}$ ). Also, from this point of view, the most natural field of PE application is the treatment of dilute solutions [2]. But this way of elevating the PE efficiency is also limited, for example, by the reduction of dissolved oxygen [20].

At high solution flow rates and the average or high concentrations of the main component, the depth of the effective working layer is small, and to provide the operation of even a thin layer a considerable current overload, attended by a noticeable decrease in the current efficiency is required. An optimal choice of the solid phase conductivity ( $\kappa_s = \kappa_L$ ) increases  $L_d$  only one and a half times. So it may be concluded that the possibilities of further increase in PE efficiency on the basis of a uniform conducting matrix are practically completely exhausted. Further progress is possible only with the application of new factors, for example, nonuniform conducting matrices [10, 21, 22].

### Acknowledgements

The authors thank the Russian Foundation for Fundamental Research for financial support of this

work (project 95-03-09661), Prof. R. Yu. Beck for useful discussion and Mrs M. Kostirya for help in the numerical calculations.

### References

- [1] I. G. Gurevitch, U. M. Volkovich and V. S. Bagotsky. 'Liquid porous electrodes', Minsk, "Nauka i tehnika" (1974), p. 245.
- [2] R. Yu. Beck, *Izvestiya SO AN SSSR*, ser. chim. nauk. vip. 6 (1977) 11.
- [3] J. Newman and W. Tiedemann, 'Advances in Electrochemistry and Electrochemical Engineering' Vol. II (edited by H. Gerischer and C. W. Tobias), Wiley-Interscience, New York (1978), p. 353.
- [4] V. S. Daniel-Beck, *Zh. Fiz. Khim.* **22** (1948) 697.
- [5] R. Alkire and A. A. Mirarefi, *J. Electrochem. Soc.* **120** (1973) 1507.
- [6] J. A. Trainham and J. Newman, *ibid.* **125** (1978) 58.
- [7] R. Yu. Beck, A. P. Zamyatin, A. N. Koshev and N. P. Poddubny, *Izvestiya SO AN SSSR*, ser. chim. nauk. vip. 2 (1980) 110.
- [8] A. N. Koshev, V. K. Varentsov and G. N. Glaiser, *Elektrokhimiya* **28** (1992) 1128.
- [9] A. I. Masliy and N. P. Poddubny, *ibid.* **27** (1991) 744.
- [10] *Idem*, *ibid.* **14** (1978) 149.
- [11] R. Yu. Beck, *Sibirskii Khim Zh.* vip. 3 (1993) 85.
- [12] N. P. Poddubny and A. I. Masliy, *ibid.*, vip. 3 (1991) 108.
- [13] R. E. Sioda, *Electrochim. Acta* **16** (1971) 1569.
- [14] A. I. Masliy and N. P. Poddubny, *Elektrokhimiya* **30** (1994) 897.
- [15] A. F. Zhrebilov and V. K. Varentsov, *Izvestiya SO AN SSSR*, ser. chim. nauk., vip. 6 (1984) 28.
- [16] G. Kreysa, *Electrochim. Acta* **23** (1978) 1351.
- [17] P. S. Fedkiw and P. S. Safemazandarani, *Chem. Engng. Commun.* **38** (1985) 107.
- [18] G. Kreysa, in 'Ullmann's Encyclopedia of Industrial Chemistry', A9 (1987) 207.
- [19] G. Kreysa, K. Jüttner and J. M. Bisang, *J. Appl. Electrochem.* **23** (1993) 707.
- [20] A. P. Zamyatin and R. Yu. Beck, *Elektrokhimiya* **20** (1984) 854.
- [21] A. I. Masliy and N. P. Poddubny, *ibid.* **29** (1993) 1166.
- [22] A. I. Masliy, N. P. Poddubny, A. Zh. Medvedev and A. V. Panasenko, *ibid.* **31** (1995) 526.